Correlation between Theory and Experiment in Electron-Transfer Reactions in Proteins: Electronic Couplings in Modified Cytochrome *c* and Myoglobin Derivatives

Prabha Siddarth[†] **and R. A. Marcus***[‡]

Department of Biochemistry, University of British Columbia, Vancouver, British Columbia, Canada V6T 1Z3, and Arthur Amos Noyes Laboratory of Chemical Physics,[§] *California Institute of Technology, Pasadena, California 91125*

Received: June 28, 1993; In Final Form: September 3, 1993[●]

The artificial intelligence–superexchange method of estimating the long-range electronic coupling in proteins that we have developed previously is used to study electron-transfer reactions in Ru-modified cytochrome *c* and myoglobin derivatives. Good correlations between theoretical and experimental rate constants are obtained using the present method. Amino acid paths for electron transfer are analyzed.

Electron-transfer (ET) reactions in proteins have been investigated in detail by several experimental groups in recent years in order to understand the factors that control the rate of these nonadiabatic reactions.[1-6] Theoretical approaches to studying such long-range ET reactions have ranged from simple tunneling methods to sophisticated path integral and quantum chemical techniques.[7-12] We have devised[10] an artificial intelligence–superexchange method to estimate the electronic coupling in long-range ET reactions such as those occurring in proteins. Previously, we have studied ET reactions within many ruthenium-modified protein derivatives (both cytochrome *c*[10] and myoglobin[13]) using this method and have estimated the electronic coupling in each of these derivatives. In the present paper, we examine three other Ru-modified cytochrome *c* derivatives, which have been experimentally investigated recently by Gray and co-workers.[14] We also review the correlations which have been obtained thus far for modified cytochrome *c* and myoglobin derivatives. The results are compared with correlations based on the pioneering atom-by-atom pathway analysis of Beratan and Onuchic.[8]

I. Theory

It is known from semiclassical ET theory[15] that the rate for a nonadiabatic ET reaction depends on a nuclear factor, which in turn depends on the driving force of the reaction ($-\Delta G^\circ$) and the extent of nuclear reorganization (λ) accompanying the electron transfer, and an electronic factor, which depends on the distance and the medium separating the electron donor and the acceptor. The rate constant is given by the product of these two factors:

$$k_{\mathrm{ET}} = \frac{2\pi}{\hbar}|H_{\mathrm{DA}}|^2(\mathrm{FC}) \tag{1}$$

where H_{DA} is the electronic coupling matrix element and FC is the Franck–Condon (nuclear) factor. In the classical limit, FC is given by

$$\mathrm{FC} = \frac{1}{(4\pi\lambda RT)^{1/2}}\exp\left(-\frac{(\Delta G^\circ + \lambda)^2}{4\lambda RT}\right) \tag{2}$$

When the driving force equals the reorganization energy, the rate constant for the ET reaction is at a maximum and is mainly controlled by the electronic coupling:

$$k_{\max} = \frac{2\pi}{\hbar}|H_{\mathrm{DA}}|^2\frac{1}{(4\pi\lambda RT)^{1/2}} \tag{3}$$

The electronic matrix element, H_{DA}, is a measure of the coupling or the interaction between the orbitals of the donor (D) and the acceptor (A). It arises from the quantum mechanical tunneling of the transferring electron through the potential energy barrier provided by the bridging medium. In the case of protein electron-transfer reactions, the intervening protein serves as the bridge. Simple square barrier tunneling models[7] yield an exponential decay of H_{DA} with the distance R separating the donor and the acceptor, when a homogeneous medium separates the two redox centers. For more complex bridging systems, the electronic structure of the bridge influences the coupling between the donor and the acceptor.

In the artificial intelligence–superexchange method,[10] the details of the electronic structure of the protein medium are taken into account in estimating the electronic coupling. The estimation of the electronic coupling proceds in two parts, the first part being an artificial intelligence (AI) search followed by a superexchange calculation. In the AI search procedure, the amino acid residues important in mediating the electron transfer between the donor and the acceptor are selected by making use of an evaluation function. The search starts from the donor atom D in the protein and travels to the acceptor atom A via the intervening atoms I of the amino acid residues of the protein molecule. The evaluation function (EF) determines which of the amino acid residues most efficiently couple the donor and the acceptor and has the following form, derived from perturbation theory:[10,13]

$$\mathrm{EF} = V_{\mathrm{DI}}T_{\mathrm{IA}}/\Delta E \tag{4}$$

where V_{DI} is a measure of the coupling of the atom I to the donor, T_{IA} is an estimate of the coupling from I to the acceptor, and ΔE is a suitably chosen energy difference. We use a different notation for the coupling of the donor atom to atom I (V_{DI}) and for the coupling of the acceptor atom to atom I (T_{IA}) in order to emphasize the V_{DI} can, in principle, be calculated exactly while T_{IA} can, by definition, only be estimated, as explained below.

The first factor in the EF, V_{DI}, is a true measure of the electronic coupling from the donor D to the intermediate atom I since the atoms involved in the path from D to I (*i.e.*, *D*, 1, 2, 3, ..., I – 1, I) are all known. Presently, we calculate V_{DI} as the product of the atom–atom couplings from D to I, divided by an energy denominator:

$$V_{\mathrm{DI}} = H_{\mathrm{D1}}\frac{H_{12}}{\Delta E}\frac{H_{23}}{\Delta E}\cdots\frac{H_{\mathrm{I-1,I}}}{\Delta E} \tag{5}$$

In the above expression, we have used identical energy denominators. Since eq 5 is used only as part of the evaluation function in the AI search and not in the final calculation of the electronic coupling matrix element (for which the superexchange expression,

---

[†] University of British Columbia.

[‡] California Institute of Technology.

[§] Contribution No. 8820.

[●] Abstract published in *Advance ACS Abstracts*, November 15, 1993.

0022-3654/93/2097-13078$04.00/0

eq 8, is utilized), we believe it is adequate to replace the exact ΔE's by some mean value, except when the actual ΔE_{IJ} is of the order of an H_{IJ}, and in that case replacing that $H_{IJ}/\Delta E_{IJ}$ by unity would be sufficient. Also, since in this formulation of the search ΔE does not depend on the particular node I, the absolute value chosen for ΔE (we currently take it to be 10 eV) does not affect the promise of a node but is incorporated here to make the usual connection to perturbation theory clear. The ΔE in eq 5 is thus different from the energy difference in the denominator of eq 8, ΔE_α, which represents the difference in energy between the donor (acceptor) orbital and the energy of the αth molecular orbital of the bridge, at the transition state. The calculation of the value of ΔE_α is discussed in a later section (section IIA).

The couplings H_{MN} between any two atoms M and N in eq 5 are themselves estimated by a modified form of the Wolfsberg–Helmholtz resonance integral between two atomic orbitals:[16]

$$H_{MN} = \max \left|KS_{mn}\left(\frac{\epsilon_m + \epsilon_n}{2}\right)\right| \tag{6}$$

where m denotes an atomic orbital on atom M, n denotes an atomic orbital on atom N, S_{mn} is the overlap integral between m and n, ϵ_m and ϵ_n are the orbital energies, and K is a constant, usually taken to be 1.75. The max in eq 6 indicates that only the mn orbital pair which gives the maximum contribution to an atom M–atom N interaction is used in the estimation of an H_{MN} for that atom–atom pair in the AI search calculation of a V_{DI}. H_{MN}, as calculated above, depends directly on the overlap between atomic orbitals. Both through-bond and through-space couplings are estimated with the above expression, which we believe is adequate for the purpose of the AI search.

The second factor in the EF, namely T_{IA}, imparts knowledge about the unexplored domain of the protein space to the search and thus transforms the search from a *blind* or *uninformed* search to a true AI or *informed* search. This factor, by definition, cannot be exactly calculated but can only be estimated. A possible estimate of this factor can be obtained by making use of the well-established empirical finding that the electronic coupling decays exponentially with distance in an average sense.[15] Therefore, we choose to estimate T_{IA} as

$$T_{IA} = C \exp(-\beta' R) \tag{7}$$

where C is a constant which represents the electronic coupling between I and A at contact distance and R is the actual distance between node I and the acceptor A. β' is the exponent which measures the rate of falloff of T_{IA}, presently taken[15] to be 0.5 Å^{-1}. We emphasize here that the expression for the evaluation function (and hence for both V_{DI} and T_{IA}) is used only for the AI search, and the actual electronic coupling matrix element H_{DA} is calculated using the superexchange formulation (eq 8).

The AI search thus uses the EF (eq 4) to proceed from one redox center to another (from D to A as well as, with V_{DI} T_{IA} replaced by V_{AI} T_{ID}, from A to D). At each step of the search, this equation is applied, and the most promising of the nodes (atoms) is selected. The search does not necessarily proceed along the backbone of the protein but instead chooses the atoms that couple in the most optimal way the donor and the acceptor, based on both overlap and energy considerations. Some number of such paths of atoms is selected from the D to A and the A to D paths (as discussed in section II.A). The amino acid residues to which these atoms belong are then regarded as the ones important in mediating the electron transfer between D and A and are accepted for use in the next part of the procedure, namely the superexchange calculation.

In the superexchange mechanism,[17] the electron makes use of the molecular orbitals of the bridge (in the present case, the subset of the protein selected by the AI search) to transfer from D to A. The molecular orbitals of the bridge and their eigenvalues are calculated separately, and the interaction of the donor/acceptor with the bridge is treated as a perturbation. The electronic coupling matrix element H_{DA} can be formulated as

$$H_{DA} = \sum_\alpha \frac{T_\alpha^D T_\alpha^A}{\Delta E_\alpha} \tag{8}$$

where T_α^D (T_α^A) represents the interaction of the donor (acceptor) orbital with the αth bridge orbital and ΔE_α is the energy of the αth bridge orbital relative to the energy of the donor orbital. (The donor and the acceptor orbitals have the same energy in the transition state.) Both occupied (hole transfer) and unoccupied (electron transfer) orbitals of the bridge are included in the summation. H_{DA} calculated using eq 8 directly depends on the electronic and molecular structure of the bridging protein medium. This perturbation approximation, which we tested earlier (see ref 25 given later) is valid when, as in the present system, ΔE_α is large compared to T_α^D and T_α^A.

The interaction of the donor D with the bridge B is given by

$$T_\alpha^D = \sum_{m_D, m_B} C_{\chi m_D}^D H_{m_D m_B} C_{m_B \alpha}^B \tag{9}$$

Similarly, T_α^A can be written as

$$T_\alpha^A = \sum_{m_B, m_A} C_{\alpha m_B}^B H_{m_B m_A} C_{m_A \mu}^A \tag{10}$$

where χ and μ denote the molecular orbitals on D and A that are involved in the electron transfer; m_D, m_B, and m_A are the atomic orbitals of D, B, and A, respectively. $H_{m_D m_B}$ are the interaction matrix elements of the donor and bridge orbitals, and $H_{m_B m_A}$ are the interaction matrix elements of the bridge and acceptor orbitals.

The energy difference in the denominator of eq 8 is given by

$$\Delta E_\alpha = E_\chi - E_\alpha \tag{11}$$

where E_α is the energy of the αth molecular orbital of B and E_χ is the energy of the molecular orbital of D, which is equal to that of A, E_μ, in the transition state. This energy is obtained from charge-transfer spectra after reorganizational correction[10,18] or, when the atoms involved in the donor/acceptor and the bridge are primarily first-row atoms, from extended Hückel theory.[13]

There has been some question or debate in k_{max}^{expt} plots as to whether distances should be measured from the center or from the edge of a reactant (e.g., ref 30, given later; also ref 14 and the two plots in the present Figure 3). In the present calculation this question does not arise as such: One requires of the quantum treatment that it give the correct election distribution on the metal atom and on the ligands, for the extra electron on the donor and, after the transfer, on the acceptor. The chosen amino acids are then used with those reactants in this quantum calculation, and a plot such as Figure 1 or 2 is then made.

II. Results and Discussion

A. Correlations between Theoretical and Experimental Rate Constants. Intraprotein ET rates were recently measured[14] in three ruthenium-modified mutants of yeast iso-1-cytochrome *c*, namely His 58, His 66, and His 66/Phe 67 (in the His 66/Phe 67 derivative, a tyrosine which is normally present at position 67 was replaced by a phenylalanine):

$$\text{Ru(III)–cyt } c\text{–Fe(II)} \rightarrow \text{Ru(II)–cyt } c\text{–Fe(III)}$$

The reorganization energy λ for the above ET reaction has been estimated to be 0.8 eV.[19] Knowing the free energies of the reaction, $\Delta G°$, for each of the three mutants enables an experimental estimate[14] of the maximum rate constant, k_{max}, and the electronic coupling matrix element, H_{DA}. For these ET reactions, the driving force of the reaction nearly equals the reorganization energy, and so the rate is mainly controlled by the electronic coupling. Hence, the "extrapolation" from k_{ET} to yield k_{max} in ref 14 is very minor.

TABLE I: Amino Acid Residues Selected by the AI Search[a]

His 66	His 66/Phe 67	His 58
His 66*	His 66*	Lys 55
Tyr 67*	Phe 67*	Val 57
Leu 68	Leu 68*	His 58*
Thr 69	Thr 69	Trp 59*
Asn 70	Asn 70	Asp 60
Pro 71	Pro 71	Asn 63
Tyr 74	Tyr 74	Met 64
Met 80*	Met 80	Ser 65
Phe 82	Phe 82	Glu 66
Wat 166		Tyr 67
		Leu 68
		Pro 71
		Tyr 74
		Ile 75
		Thr 78
		Lys 79
		Met 80

[a] Amino acid residues labeled with an asterisk are the ones found int he "best" path.

In the theoretical procedure for estimating the electronic coupling, the known structure of wild-type yeast iso-1-cytochrome *c* was modified with a Ru(bpy)$_2$(im)(His) group at positions 58 and 66 to yield the Ru His 58 and Ru His 66 derivatives, respectively, and the known structure of the Phe 67 mutant was modified with the same group at position 66 to obtain the Ru His 66/Phe 67 derivative.[20] A conformational search of the Ru-modified histidine side-chain dihedral angles was then performed on each of these derivatives to determine the most stable conformer.[21] The coordinates of these minimized structures were then used in the AI search.

As outlined in section I, the AI search was used to extract a subset of important amino acid residues for each derivative (Table I). The two metal atoms (*i.e.*, the Fe in the heme of the protein and the Ru in the Ru(bpy)$_2$(im)(His) group) were taken as the donor and the acceptor, respectively. During the course of the search, many paths from the donor to the acceptor (as well as from the acceptor to the donor) are evaluated, and all those paths which have a net electronic interaction greater than a threshold value[22] are accepted. The amino acid residues which form these paths constitute the desired subset for each derivative. Only this limited subset (10–20 from a total of 108 amino acid residues present in cytochrome *c*) is used in the superexchange calculation.

The electronic coupling matrix element for each derivative was then calculated by determining the molecular orbital coefficients C^D, C^B, and C^A, the interaction matrix elements $H_{m_Dm_B}$ and $H_{m_Bm_A}$, and the eigenvalues E_α of the bridge using extended Hückel theory.[23] In order to determine the donor (acceptor) energy relative to the bridge orbitals at the transition state, the absorption spectrum maximum associated with charge transfer from porphyrin to metal in ferricytochrome *c* was used, as discussed in a previous article.[24] From the calculated H_{DA}'s, the maximum rate constants k_{max}^{calc} were obtained using eq 3.

The results of the present study of modified cytochrome *c* derivatives, together with those given earlier,[10] are presented in Figure 1. They are compared there with the maximum rate constants k_{max}^{expt}, inferred from experimental data.[14] The corresponding results obtained earlier (but represented in a different way) for modified myoglobin derivatives[13] are given in Figure 2. In both cases, there is seen to be a smooth correlation between calculated and experimental k_{max}'s, though the slopes of the log–log plots differ from the value of unity. (The slopes are 0.54 for Figure 1 and 1.27 for Figure 2.) The origin of these deviations remains to be determined. For the myoglobin derivatives, the deviation of the slope is close to the range (10–25%) found for the rigid-bridged compounds.[18,25] However, it is desirable to have additional points before making a definitive judgement. The intercepts of the plots are also not equal to the ideal value of zero; the intercepts are a measure of both the variation of the rate constants within the protein and the agreement of the absolute values of the experimental and theoretical rate constants. Given the semiempirical nature of extended Hückel theory, it is not possible to obtain more than an order of magnitude agreement between the measured and calculated values.

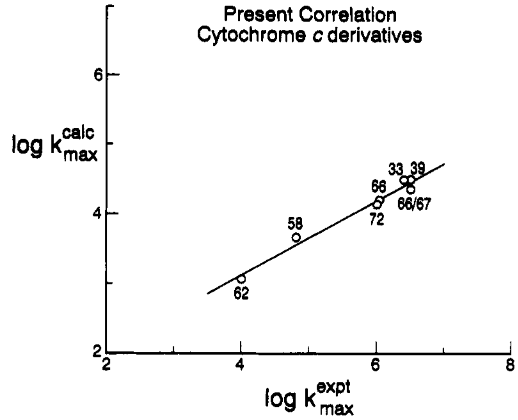

Figure 1. Correlation of experimental and calculated rate constants for Ru-modified cytochrome *c* derivatives. The calculated results for the His 66, His 66/Phe 67, and His 58 derivatives are from present work, while those for His 33, His 39, His 72, and His 62 are from ref 10. The experimental rate constants have been taken from ref 14.

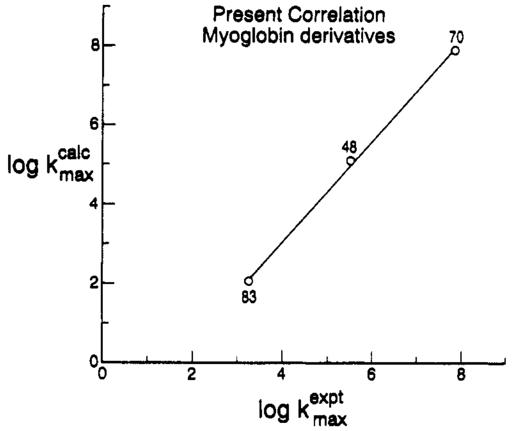

Figure 2. Correlation of experimental and calculated rate constants for Ru-modified myoglobin derivatives. The calculated rate constants are from ref 13, and the experimental rate constants are from ref 1.

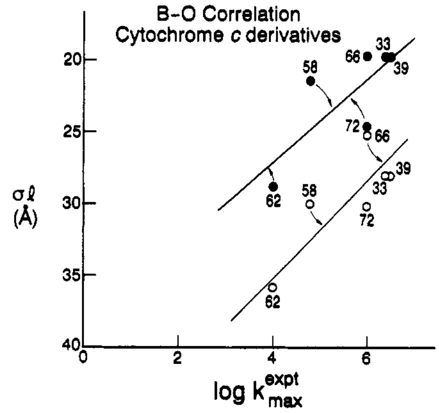

Figure 3. Correlation of experimental rate constants with B–O σ-tunneling lengths σ*l* for Ru-modified cytochrome *c* derivatives (ref 14). The filled circles refer to the edge–edge σ-tunneling results, and the open circles refer to the Ru–Fe σ-tunneling results.

The results obtained using the Beratan–Onuchic (B–O) method[8] are given, for comparison, in Figures 3 and 4. In Figure 3, the correlations obtained using both the edge–edge and Ru–Fe σ-tunneling lengths[14] have been plotted, while in Figure 4 the two correlations plotted were obtained using single pathway and

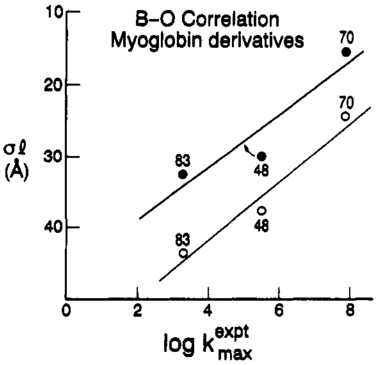

Figure 4. Correlation of experimental rate constants with B–O σ-tunneling lengths σl for Ru-modified myoglobin derivatives (ref 1). The filled circles refer to the (edge–edge) multiple pathway results, and the open circles refer to the single pathway results.

multiple pathway σ-tunneling lengths.[1] Instead, it is also possible to use as the ordinate in Figures 3 and 4 the log k^{calc}_{max} calculated from the B–O σ-tunneling lengths. The correlations in the B–O rate plots are identical with those in the σ-tunneling length plots given here. Since the B–O method does not provide the prefactors (*i.e.*, the interaction between the donor (acceptor) with the first (last) bond of the pathway) necessary to calculate *absolute* values of H_{DA} and k_{max}, only comparisons of *relative* coupling strengths and rates of ET reactions within a given series are valid.

With the body of results presented in Figures 1–4, it is useful to make some comparison of the two methods. The two methods have different aims and can be regarded as complementary. The atom-by-atom path method of Beratan and Onuchic is a pioneering method and has the real virtue of simplicity. Its limitations are also contained in that simplicity: There is a separate parameter for each mode of travel (through any type of covalent bond, through a hydrogen bond, and through space). The atom–atom interaction is also too large to be treated literally by a path method, if the justification used for the path method is the usual one of perturbation theory.[18] Beratan and Onuchic have proposed[8] that the decay factor across a bond can be viewed as a renormalized parameter which can take into account the effect of side groups and backscattering. However, in all the implementations of the B–O method so far, only a uniform decay parameter of 0.6 for all types of covalent bonds has been used.

The present method is seen to yield less scatter (Figures 1 and 2) than that in Figures 3 and 4, and in addition, it contains no adjustable parameters.[26] The correlation coefficients for the least-squares line in Figures 1 and 2 are both 0.99, while in Figure 3 the correlation coefficients are 0.78 and 0.82 and in Figure 4 they are 0.98 and 0.93 for the two sets of correlations shown there. In order to make predictions using any correlation, it is desirable to have as small a scatter as possible, *i.e.*, a correlation coefficient of close to unity.[27] Any change in the B–O parametrization factor[8] of 0.6 (or the inclusion of prefactors to calculate k^{calc}_{max} for the B–O method) influences the absolute values of the B–O σ-tunneling lengths (and hence the k^{calc}_{max}) but does not affect the scatter in Figures 3 and 4 or their correlation coefficients. The present method can also be legitimately visualized in terms of a path or paths of *amino acid residues*, since this procedure was justified elsewhere by perturbation theory.[18] While not difficult to implement, it is, on the other hand, more complicated than the Beratan–Onuchic approach. Nevertheless, it can be expected to be replaced by more accurate methods, perhaps retaining some of the features of the present method such as the "molecule in protein" approach (amino acid fragments) and the informed AI search.

B. Amino Acid Paths. The calculated electronic matrix elements for the three derivatives presently studied are given in Table II and are compared there with the experimental estimates of H_{DA}. The His 66/Phe 67 mutant shows similar coupling to the His 66 derivative containing the Tyr 67 (a slight increase in H_{DA} by a factor of 1.2), even though replacement of tyrosine with a phenylalanine is expected to create a gap between Phe 67 and Met 80 and to reduce the coupling. Gray and co-workers have speculated[14] that an additional internal water molecule, present in the Phe 67 mutant,[28] could help in the coupling of the Phe 67 to Met 80. (Pathway results for the Phe 67 mutant are not available.) Presently, this internal water molecule is not selected by the AI search. Hence, according to the evaluation function used, this water molecule is not found to be important for this electron-transfer reaction. Further, we then examined the effect of including the water molecule in the superexchange calculation. Relatively little change in the value of H_{DA} resulted (from 9×10^{-3} to 8×10^{-3} cm^{-1}).

TABLE II: Calculated and Experimental Electronic Coupling Matrix Elements

	H_{DA} (cm^{-1})	
derivative	calc[a]	expt[b]
His 66	7.5×10^{-3} (9.0×10^{-3})	6.0×10^{-2}
His 66/Phe 67	9.0×10^{-3} (8.4×10^{-3})	1.0×10^{-1}
His 58	4.0×10^{-3} (4.7×10^{-3})	1.4×10^{-2}

[a] The values in parentheses are the results obtained for the "best" path calculation. [b] Reference 14.

In order to understand the nature of the electronic coupling in the Phe 67 mutant, we considered the "best" amino acid path determined from the AI search, *i.e.*, the amino acid path with the greatest net electronic interaction as estimated from the evaluation function. For the His 66 derivative containing the Tyr 67, the amino acid residues in the best path are His 66, Tyr 67, and Met 80, while for the Phe 67 mutant, His 66, Phe 67, and Leu 68 are the amino acid residues in the best path. A calculation of the electronic coupling using only these residues as the bridge gives H_{DA} values of 9×10^{-3} and 8.4×10^{-3} cm^{-1} for the His 66 and the His 66/Phe 67 derivatives, respectively, as compared with the values of 7.5×10^{-3} and 9.0×10^{-3} cm^{-1}, respectively, for the full calculation. These results indicate that replacement of Tyr 67 with a Phe could cause a change in the dominant amino acid path for ET and still lead to similar electronic coupling. However, it is to be noted that the internal water molecule is found to have a high thermal factor in the crystallographic analysis of the Phe 67 mutant,[29] and it is possible that at other positions sampled by the water molecule, not the position from the crystal structure upon which the present calculations were based, this water molecule could play a role in enhancing the coupling for the Phe 67 mutant.

While the artificial intelligence search is able to specify the amino acid residues involved in the electron transfer, the superexchange calculation reveals the nature of the bridge (amino acid) orbitals that are important in the electron-transfer event. It is found that although both occupied and unoccupied orbitals of the amino acid residues play a role, it is predominantly the occupied orbitals that contribute significantly to the electronic coupling. For the three derivatives studied presently, hole transfer accounts for more than 80% of the electronic coupling matrix element. This is primarily due to the proximity of their energy values to the energy of the donor (acceptor) orbital. For the orbitals closest in energy to the donor orbital, typical values of ΔE_α are about 1.0 eV while the magnitude of the interaction T^D_α or T^A_α is about 2×10^{-2} eV or less, thus satisfying the perturbation approximation inherent in the superexchange formalism.

III. Conclusions

In the present paper, we have studied the electronic coupling provided by the protein medium in long-range ET reactions of cytochrome *c*. The theoretical model used, namely the AI-superexchange method, not only yields values of electronic coupling in agreement with experimental data but also provides insight into the nature of the important amino acid paths for ET. The current state of correlations of experimental and calculated rate constants for both cytochrome *c* and myoglobin derivatives is described.

Acknowledgment. It is a pleasure to acknowledge the support of this research by the National Science Foundation and by the Office of Naval Research. This article is dedicated to the memory of Gerhard Closs, whose pioneering experiments played a major role in our own work and whose friendship and insight we shall always remember. We appreciate the useful comments of Jose Onuchic and David Beratan on this article. P.S. thanks Gary Brayer, Albert Berghuis, Terence Lo, and Danny Casimiro for helpful discussions and the authors of ref 14 for their preprint. This work is supported in part by the Caltech–JPL CRAY Supercomputing Project. Use of the Canadian Protein Engineering National Centers of Excellence Computational Center in Gary Brayer's laboratory at UBC is gratefully acknowledged.

References and Notes

(1) Casimiro, D. R.; Wong, L.-L.; Colon, J. L.; Zewert, T. E.; Richards, J. H.; Chang, I.-J.; Winkler, J. R.; Gray, H. B. *J. Am. Chem. Soc.* **1993**, *115*, 1485.

(2) Corin, A. F.; Hake, R. A.; McLendon, G.; Hazzard, J. T.; Tollin, G. *Biochemistry* **1993**, *32*, 2756.

(3) Govindaraju, K.; Christensen, H. E. M.; Lloyd, E.; Olsen, M.; Salmon, G. A.; Tomkinson, N. P.; Sykes, A. G. *Inorg. Chem.* **1993**, *32*, 40.

(4) Farver, O.; Pecht, I. *J. Am. Chem. Soc.* **1992**, *114*, 5764. Farver, O.; Skov, L. K.; Pascher, T.; Karlsson, B. G.; Nordling, M.; Lundberg, L. G.; Vänngard, T.; Pecht, I. *Biochemistry* **1993**, *32*, 7317.

(5) Nocek, J. M.; Stemp, E. D. A.; Finnegan, M. G.; Koshy, T. I.; Johnson, M. K.; Margoliash, E.; Mauk, A. G.; Smith, M.; Hoffman, B. M. *J. Am. Chem. Soc.* **1991**, *113*, 6822.

(6) Willie, A.; Stayton, P. S.; Sligar, S. G.; Durham, B.; Millett, F. *Biochemistry* **1992**, *31*, 7237.

(7) DeVault, D. *Quantum-Mechanical Tunneling in Biological Systems*; Cambridge University Press: Cambridge, 1984.

(8) Betts, J. N.; Beratan, D. N.; Onuchic, J. N. *J. Am. Chem. Soc.* **1992**, *114*, 4043. Onuchic, J. N.; Beratan, D. N.; Winkler, J. R.; Gray, H. B. *Annu. Rev. Biophys. Biomol. Struct.* **1992**, *21*, 349. Onuchic, J. N.; Beratan, D. N. *J. Chem. Phys.* **1990**, *92*, 722. Beratan, D. N.; Onuchic, J. N.; Hopfield, J. J. *J. Chem. Phys.* **1987**, *86*, 4488.

(9) Kuki, A.; Wolynes, P. G. *Science* **1987**, *236*, 1647. Gruschus, J. M.; Kuki, A. *J. Phys. Chem.* **1993**, *97*, 5581.

(10) Siddarth, P.; Marcus, R. A. *J. Phys. Chem.* **1993**, *97*, 2400.

(11) Braga, M.; Larsson, S. *Int. J. Quantum Chem.* **1992**, *44*, 839.

(12) Liang, C.; Newton, M. D. *J. Phys. Chem.* **1992**, *96*, 2855.

(13) Siddarth, P.; Marcus, R. A. *J. Phys. Chem.* **1993**, *97*, 6111. The donor and the acceptor in the myoglobin derivatives are the Zn porphyrin group and the ruthenated histidine group, respectively.

(14) Casimiro, D. R.; Richards, J. H.; Winkler, J. R.; Gray, H. B. *J. Phys. Chem.*, submitted.

(15) Marcus, R. A.; Sutin, N. *Biochim. Biophys. Acta* **1985**, *811*, 265.

(16) Wolfsberg, M.; Helmholtz, L. *J. Chem. Phys.* **1952**, *20*, 837.

(17) Halpern, J.; Orgel, L. E. *Discuss. Faraday Soc.* **1960**, *29*, 32. McConnell, H. M. *J. Chem. Phys.* **1961**, *35*, 508.

(18) Siddarth, P.; Marcus, R. A. *J. Phys. Chem.* **1992**, *96*, 3213.

(19) Wuttke, D. S.; Bjerrum, M. J.; Winkler, J. R.; Gray, H. B. *Science* **1992**, *256*, 1007. Wuttke, D. S.; Bjerrum, M. J.; Chang, I.-J.; Winkler, J. R.; Gray, H. B. *Biochim. Biophys. Acta* **1992**, *1101*, 168.

(20) The coordinates of wild-type yeast iso-1-cytochrome *c* (Louie, G. V.; Brayer, G. D. *J. Mol. Biol.* **1990**, *214*, 527) and the Phe 67 mutant (Berghuis, A. M.; Guillemette, J. G.; Smith, M.; Brayer, G. D. *J. Mol. Biol.*, in press) were kindly provided by Gary Brayer. Molecular modeling was done using Insight, Version 2.2.0, on a Silicon Graphics Power Station 440VGX.

(21) The two side-chain dihedral angles C_α–C_β and C_β–C_γ were each rotated by 1° from 0° to 360°, *i.e.*, for each value of the C_α–C_β angle, the C_β–C_γ angle was rotated by 1° from 0° to 360°. Thus, a total of 360 × 360 conformations were searched.

(22) The threshold values used were 10^{-14} for the His 66 and His 66/Phe 67 derivatives and 10^{-16} for the His 58 derivative.

(23) QCPE Program No. 517, Indiana University, Bloomington, IN. The basis set and valence state ionization energies for the metal atoms were obtained from QCPE Program No. 387.

(24) See Appendix I of ref 10. The value of the donor energy obtained by this method is –10.68 eV, which is equal to the energy of the acceptor orbital at the transition state.

(25) Siddarth, P.; Marcus, R. A. *J. Phys. Chem.* **1990**, *94*, 2985.

(26) Molecular orbital calculations using extended Hückel theory involve a constant K in the off-diagonal Hamiltonian matrix element H_{ab}, which is given by $KS_{ab}(H_{aa} + H_{bb})/2$. This constant K is usually taken to be 1.75 (see: Boca, R.; Pelikan, P. *Coord. Chem. Rev.* **1992**, *118*, 1. Lowe, J. P. *Quantum Chemistry*; Academic Press: New York, 1978), as was done in all our studies.

(27) Hays, W. L. *Statistics*; Dryden Press: 1988. A definition of the correlation coefficient appears in eq 14.4.5, p 555.

(28) In the Phe 67 mutant, in addition to Wat 166 which is present in both the wild-type yeast iso-1-cytochrome *c* and the Phe 67 mutant structures, an extra water molecule (Wat 300) is found in the crystallographic structure analysis (McLendon, G.; Hickey, D.; Berghuis, A.; Sherman, F.; Brayer, G. *ACS Adv. Chem. Series*, Vol. 228; Bolton, J. R., Mataga, N., McLendon, G.; Eds.; American Chemical Society: Washington, DC, 1991; p 179; see also ref 29).

(29) Berghuis, A. M.; Guillemette, J. G.; Smith, M.; Brayer, G. D. *J. Mol. Biol.*, in press.

(30) Farid, R. S.; Moser, C. C.; Dutton, P. L. *Curr. Opin. Struct. Biol.* **1993**, *3*, 225.